JVI Journals.ASM.org

Improving Neutralization Potency and Breadth by Combining Broadly Reactive HIV-1 Antibodies Targeting Major Neutralization Epitopes

Rui Kong,[a] Mark K. Louder,[a] Kshitij Wagh,[b] Robert T. Bailer,[a] Allan deCamp,[c] Kelli Greene,[d] Hongmei Gao,[d] Justin D. Taft,[a] Anna Gazumyan,[e] Cassie Liu,[e] Michel C. Nussenzweig,[e,f] Bette Korber,[b] David C. Montefiori,[d] John R. Mascola[a]

Vaccine Research Center, NIAID, NIH, Bethesda, Maryland, USA[a]; Theoretical Division, Los Alamos National Laboratory, Los Alamos, New Mexico, USA[b]; Fred Hutchinson Cancer Research Center, Seattle, Washington, USA[c]; Departments of Surgery and Immunology, Duke University Medical Center, Durham, North Carolina, USA[d]; Laboratory of Molecular Immunology, The Rockefeller University, New York, New York, USA[e]; Howard Hughes Medical Institute, The Rockefeller University, New York, New York, USA[f]

ABSTRACT

The isolation of broadly neutralizing HIV-1 monoclonal antibodies (MAbs) to distinct epitopes on the viral envelope glycoprotein (Env) provides the potential to use combinations of MAbs for prevention and treatment of HIV-1 infection. Since many of these MAbs have been isolated in the last few years, the potency and breadth of MAb combinations have not been well characterized. In two parallel experiments, we examined the *in vitro* neutralizing activities of double-, triple-, and quadruple-MAb combinations targeting four distinct epitopes, including the CD4-binding site, the V1V2-glycan region, the V3-glycan supersite, and the gp41 membrane-proximal external region (MPER), using a panel of 125 Env-pseudotyped viruses. All MAb combinations showed substantially improved neutralization breadth compared to the corresponding single MAbs, while the neutralization potency of individual MAbs was maintained. At a 50% inhibitory concentration (IC_{50}) cutoff of 1 μg/ml per antibody, double-MAb combinations neutralized 89 to 98% of viruses, and triple combinations neutralized 98 to 100%. Overall, the improvement of neutralization breadth was closely predicted by an additive-effect model and explained by complementary neutralization profiles of antibodies recognizing distinct epitopes. Subtle but consistent favorable interactions were observed in some MAb combinations, whereas less favorable interactions were observed on a small subset of viruses that are highly sensitive to V3-glycan MAbs. These data demonstrate favorable *in vitro* combinations of broadly neutralizing HIV-1 MAbs and suggest that such combinations could have utility for HIV-1 prevention and treatment.

IMPORTANCE

Over the last 5 years, numerous broadly reactive HIV-1-neutralizing MAbs have been isolated from B cells of HIV-1-infected donors. Each of these MAbs binds to one of the major vulnerable sites (epitopes) on the surface of the viral envelope glycoprotein. Since antibodies to distinct viral epitopes could theoretically act together to provide greater potency and breadth of virus neutralization, we tested physical mixtures of double, triple, and quadruple combinations of neutralizing MAbs targeting four major epitopes on HIV-1 Env. When tested together, antibody combinations showed substantially improved neutralization breadth compared to single MAbs. This improvement could be explained by the complementary neutralization profiles of individual MAbs. We further demonstrated that each antibody maintained its full neutralization potency when used in combination with other MAbs. These data provide a rationale for clinical use of antibody-based combinations for HIV-1 prevention and therapy.

Eliciting broadly neutralizing antibodies through immunization is a major goal of human immunodeficiency virus type 1 (HIV-1) vaccine development. However, vaccine immunogens that can induce such antibodies are not yet available (1–5). Over the last 5 years, advances in antigen-specific cell sorting of memory B cells (6, 7) and improved culture methods for single B cells (8–11), together with genetic recovery of antibody variable regions (12, 13), have resulted in the isolation of numerous highly potent and broadly reactive monoclonal antibodies (MAbs) from HIV-1-infected individuals (7–11, 14–37). Characterization of these antibodies has uncovered four main sites of vulnerability on the viral envelope glycoprotein spike (Env): the CD4-binding site (CD4bs) (7, 11, 15–21, 37), a glycan-dependent site in variable region 3 (V3) of gp120 (9, 14, 22–25), a variable-region (V1V2) glycan-dependent site on the trimer apex (8, 9, 26–31), and the membrane-proximal external region (MPER) of gp41 (10, 32–36). Recently, antibodies to an additional conserved neutralization epitope that bridges gp120 and gp41 have also been described (38–41). The isolation and characterization of these various broadly neutralizing MAbs provide templates for rational HIV-1 vaccine design and have facilitated an understanding of the im-

Received 30 October 2014 **Accepted** 9 December 2014

Accepted manuscript posted online 17 December 2014

Citation Kong R, Louder MK, Wagh K, Bailer RT, deCamp A, Greene K, Gao H, Taft JD, Gazumyan A, Liu C, Nussenzweig MC, Korber B, Montefiori DC, Mascola JR. 2015. Improving neutralization potency and breadth by combining broadly reactive HIV-1 antibodies targeting major neutralization epitopes. J Virol 89:2659–2671. doi:10.1128/JVI.03136-14.

Editor: G. Silvestri

Address correspondence to David C. Montefiori, monte@duke.edu, or John R. Mascola, jmascola@nih.gov.

R.K. and M.K.L. contributed equally to this article.

Supplemental material for this article may be found at http://dx.doi.org/10.1128/JVI.03136-14.

Copyright © 2015, American Society for Microbiology. All Rights Reserved.

doi:10.1128/JVI.03136-14

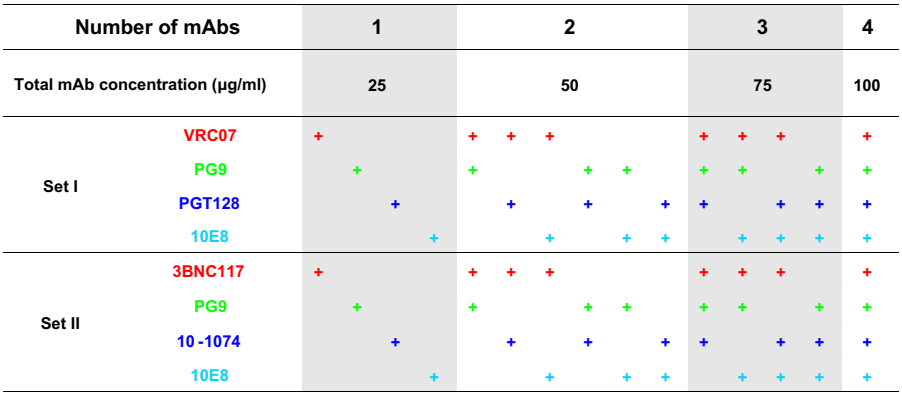

FIG 1 Experimental design of *in vitro* MAb combinations. Broadly neutralizing MAbs were combined in equal concentrations and tested for HIV-1 neutralization. Two sets of experiments (set I and set II) were performed. The number of MAb components and the total starting antibody concentration in the neutralization assays are shown, i.e., when single MAbs were tested, the starting total antibody concentration was 25 μg/ml; when two MAbs were mixed together, the total starting concentration was 50 μg/ml (25 μg/ml of each MAb), and similarly for the combinations of three and four MAbs. The MAb components of each combination are shown in red for the CD4bs MAbs VRC07 and 3BNC117, green for the V1V2-glycan MAb PG9, blue for the V3-glycan MAbs PGT128 and 10-1074, and light blue for the gp41-MPER MAb 10E8.

mune pathways leading to the development of broadly neutralizing antibodies (17, 18, 26, 42, 43). In addition to these vaccine implications, there is the potential for clinical use of MAbs by passive transfer for prevention and treatment of HIV-1 infection.

Passive immunization with HIV-1-neutralizing antibodies has provided complete protection against lentiviral infection in several studies using different animal models, including chimeric simian-human immunodeficiency virus (SHIV) challenge of rhesus macaques (44–50) and HIV-1 challenge of humanized mice (51, 52). Additionally, passive delivery of HIV-1 MAbs has been assessed for efficacy as immunotherapy. Early animal and human studies showed a limited and transient impact on viremia and rapid emergence of neutralization-resistant variants after antibody administration (53–56). Recently, using the newly isolated MAbs, which are more potent and broadly reactive, several animal studies demonstrated a substantial decrease in plasma viremia as long as antibodies were present, including complete control of viremia in some cases, especially when combinations of MAbs were used (49, 57, 58).

The recent resolution of the structure of the native Env trimer (59–61), together with the crystal structures of liganded MAbs (10, 14, 15, 19–24, 26–31, 35, 36, 62), has provided an understanding of the modes of recognition of most major MAbs. These data suggest that, in most cases, MAbs to distinct epitopes should bind the Env trimer without cross-competition. Likewise, *in vitro* binding data have confirmed the independent binding of distinct MAbs (26, 41). Based on the assumption that antibodies targeting different epitopes should act additively when combined, the percentage of diverse viruses neutralized (virus coverage) by MAb combinations has been predicted to be greater than that neutralized by a single MAb (9). Prior studies of recently isolated HIV-1-neutralizing MAbs have evaluated physical mixtures of two antibodies. One study tested the combination of antibodies to the CD4-binding site and the V1V2-glycan region on a panel of 208 viruses (63), and another tested the combination of the CD4-binding site and V3-glycan-directed MAbs on a panel of 45 viruses (64). Both studies showed improved virus coverage by the MAb combination. However, the potency and breadth of the combination of MAbs targeting all four main neutralization epitopes have not been well characterized experimentally. In this study, we examined the *in vitro* neutralizing activity of double, triple, and quadruple combinations of antibodies targeting four vulnerable sites on a panel of 125 HIV-1 Env-pseudotyped strains in a single-round infection assay. The results indicated nearly 100% neutralization coverage by MAb combinations plus subtle but consistent nonadditive potency interactions (favorable and less favorable) observed in some combinations.

MATERIALS AND METHODS

Combinations of MAbs. Six human MAbs (VRC07, PG9, PGT128, 10E8, 3BNC117, and 10-1074) were expressed as IgG1 and purified through a protein A column as described previously (26). All the MAbs were isolated from HIV-1-infected individuals (7–10, 14, 15, 37, 52). In this study, four MAbs (VRC07, PG9, PGT128, and 10E8) were included in set I combinations. In set II combinations, VRC07 and PGT128 were replaced by 3BNC117 and 10-1074. In each set, a total of 6 double-, 4 triple-, and 1 quadruple-MAb mixtures were made by combining MAbs at equal concentrations (Fig. 1). Therefore, all possible combinations were covered. Of note, VRC07 (37), PG9 (8, 65), PGT128 (9), and 10E8 (10) did not show substantial polyreactivity in previous reports, while 3BNC117 showed some polyreactivity (15).

Viruses. A multiclade panel of 125 HIV-1 Env-pseudotyped strains was used for MAb neutralization. The panel is a subset of a larger panel of HIV-1 Env reference strains ($n = 219$) described previously (66). It includes 11 clade A, 22 clade B, 38 clade C, 5 clade D, 16 CRF01-AE, 7 clade G, 9 CRF02-AG, and another 17 varied recombinant strains. The set also includes 31 transmitted/founder (T/F) viruses.

Neutralization assays. We used an automated 384-well microneutralization assay to quantitatively evaluate the neutralizing activity of MAbs, as described previously (67, 68). Each MAb or MAb combination was assayed at 5-fold dilutions starting at 25 μg/ml of each MAb component, i.e., when single MAbs were tested, the starting total MAb concentration was 25 μg/ml, while the starting total concentration of double-MAb combinations was 50 μg/ml (25 μg/ml of each MAb) (Fig. 1). The neutralization titers (50% inhibitory concentrations [IC_{50}s]) of all MAb combinations in this study were calculated according to the concentration of each MAb component, i.e., an IC_{50} of 1 μg/ml for the MAb combination VRC07-PG9 indicates 1 μg/ml of VRC07 plus 1 μg/ml of PG9.

P-B curves. Using the IC_{50}s of each single MAb and MAb combination, potency-breadth (P-B) curves were generated with GraphPad Prism version 6.0c.

Heat maps. Heat maps were implemented in R or Python. The heat maps illustrating coverage were generated using the heat map tool at the Los Alamos HIV database (http://www.hiv.lanl.gov/content/sequence/HEATMAP/heatmap.html), with envelopes organized according to like behavior in terms of neutralization susceptibility using hierarchical clustering. Specifically, a threshold IC_{50} (or IC_{80}) value of 25 μg/ml was set for neutralization responses that were below the level of detection in the assay, and these were highlighted in blue; complete linkage clustering of Euclidean distances between pairwise comparisons of $\log_{10}$ IC_{50} (or $\log_{10}$ IC_{80}) Env susceptibilities was used to organize the rows. The antibody columns were organized to reflect the experimental design.

sCD4 and 17b neutralization. As a positive control exemplifying a well-established synergy scenario, MAb 17b, which recognizes a CD4-induced (CD4i) epitope, was combined with soluble CD4 (sCD4) at equal molar concentrations. The single MAb 17b, sCD4, and a combination of the two were tested in parallel for neutralization on a panel of 195 HIV-1 Env-pseudotyped viruses. The assay was performed at a starting concentration of 500 nM of the single MAb 17b alone or sCD4 alone or with a combination of the two reagents consisting of 500 nM each. A total of eight viruses (HXB2.DG, MN.3, SF162.LS, CNE40, MW965.26, 57128.vrc15, UG021.16, and UG024.2) were neutralized with measurable IC_{50}s for both 17b and sCD4. Therefore, the interaction scores of the sCD4-17b combination were calculated based on IC_{50} data generated from the viruses.

IC_{50} predictions for MAb combinations. Assuming combinations of antibodies were additive, given the law of mass action, the experimental design, and the fact that an IC_{50} is an inverse measure of effectiveness, we predicted the neutralization titers (IC_{50}s) of MAb combinations using the following formulas: a and $b = 1/(1/a + 1/b)$, a and b and $c = 1/(1/a + 1/b + 1/c)$, and a and b and c and $d = 1/(1/a + 1/b + 1/c + 1/d)$, where a, b, c, and d are the IC_{50}s of the single MAb.

Of note, only viruses with measurable IC_{50}s, i.e., IC_{50}s of <25 μg/ml, of all component MAbs are qualified for this approach. For example, 71 out of 125 viruses are sensitive to neutralization by VRC07 and PGT128 when tested alone, so the IC_{50} of the VRC07-PGT128 combination was predicted based on these 71 viruses (see Fig. 7A). Similarly, the IC_{50} of the PG9-10E8 combination was predicted based on 105 out of the 125 viruses (see Fig. 7B).

Analysis of the combination effect. To determine if the combination effect was different from the prediction based on an additive model, we defined an interaction score to compare the experimental IC_{50} to the predicted IC_{50} using the following formula: interaction score = $\log_{10}$ (predicted IC_{50}/experimental IC_{50}).

Thus, a positive score indicates an experimental IC_{50} that was lower than predicted, i.e., the combination is more potent than predicted by the additive model, while a negative score indicates that the combination is less potent than predicted by the additive model. For each MAb combination, the interaction scores were calculated based on all viruses that were qualified for IC_{50} prediction. The mean value and the 95% confidence interval (CI) of interaction scores were also determined for each combination. Notably, this method is mathematically similar to the previously reported Chou-Talalay methods (69). The graphics and statistical tests mentioned in the text were implemented in R.

Statistics. R (http://www.r-project.org/) was used to calculate the Pearson's product moment correlation coefficient and the linear fit.

RESULTS

Experimental design of MAb combinations. To characterize the effect of combining broadly neutralizing MAbs with distinct epitopes on HIV-1 neutralization, we examined single, double, triple, and quadruple combinations of MAbs that target four vulnerable sites on the HIV-1 Env trimer. They included the CD4-binding site MAbs VRC07 (37, 52) and 3BNC117 (15), the V1V2-glycan-directed MAb PG9 (8), the V3-glycan supersite-directed MAbs PGT128 and 10-1074 (9, 14), and the gp41 MPER MAb 10E8 (10). Two sets of MAb combinations were designed. Each set contained four MAbs covering each of the four vulnerable sites. Set I contained VRC07, PG9, PGT128, and 10E8. Due to their potential clinical development, set II substituted 3BNC117 for VRC07 and 10-1074 for PGT128 (Fig. 1). In order to cover all possible mixtures within each set, we combined the four MAbs into 11 total combinations (6 pairs, 4 triplets, and 1 quadruplet) at equal component concentrations. The MAb mixtures and the corresponding individual MAbs were then tested in parallel for neutralization against a panel of 125 HIV-1 Env pseudovirus strains. Virus neutralization by a single MAb was performed at a starting concentration of 25 μg/ml, whereas the neutralization by MAb combinations was performed at a starting concentration of 25 μg/ml of each MAb component. Thus, the total starting antibody concentration for double-, triple-, and quadruple-MAb combinations were 50, 75, and 100 μg/ml, respectively. This approach was taken to simulate the maximum potential for passive immunization with MAb combinations, i.e., infusing two or more antibodies simultaneously for prevention or treatment of HIV-1 infection.

Experimental reproducibility. Since the neutralizing activities of PG9, 10E8, and the PG9-10E8 combination were assessed on the full panel of 125 viruses independently in set I and II experiments, we compared the repeat IC_{50} data for evaluation of reproducibility. The repeat IC_{50}s for MAbs PG9 and 10E8 individually, and when mixed together, showed strong correlation, as indicated by the close overlap of the experimental and ideal regression lines (Fig. 2). Highly significant correlations were observed in all three cases: the single MAb PG9 (Pearson $R = 0.98$; $P < 2.2 \times 10^{-16}$), the single MAb 10E8 (Pearson $R = 0.90$; $P < 2.2 \times 10^{-16}$), and the PG9-10E8 combination (Pearson $R = 0.93$; $P < 2.2 \times 10^{-16}$). These results indicated high reproducibility of the experimental data in this formally optimized and validated 384-well automated assay (67, 68).

MAb combinations showed improved neutralization breadth. To evaluate the neutralization activities of individual MAbs and their combinations, P-B curves were generated by graphing the fraction of HIV-1 strains neutralized versus an IC_{50} cutoff value (Fig. 3). For each of the individual MAbs, the P-B curves were consistent with previously published results (7–10, 37). Notably, the V3-glycan MAbs PGT128 and 10-1074 had a maximum breadth of ~60% but were highly potent on the viruses neutralized. This can be seen as a shift to the left on P-B curves (Fig. 3) and as low geometric mean IC_{50} and IC_{80} values calculated on the subset of neutralized viruses (Fig. 4). MAb PG9 neutralized almost 80% of the viruses, and the CD4bs MAbs VRC07 and 3BNC117 each neutralized about 90% of the viruses. These V1V2-glycan and CD4bs MAbs were potently neutralizing, though somewhat less potent than 10-1074 and PGT128. MAb 10E8 neutralized the greatest fraction of viruses (>95%) but with a somewhat lower potency than the other MAbs. Several prior publications estimated the breadth of coverage for MAb combinations by using individual MAb data and plotting the theoretical coverage, or theoretical P-B curve, of a combination of two MAbs, i.e., for any given virus, the smaller of the two IC_{50}s was used to plot the curve (9, 63). Thus, the breadth of coverage at a given IC_{50} cutoff value (e.g., 10 μg/ml) represents the predicted coverage if each antibody was present at 10 μg/ml. In this study, we performed neutralization assays on a panel of 125 viruses with the physical combinations of antibodies and can therefore compare the experimental

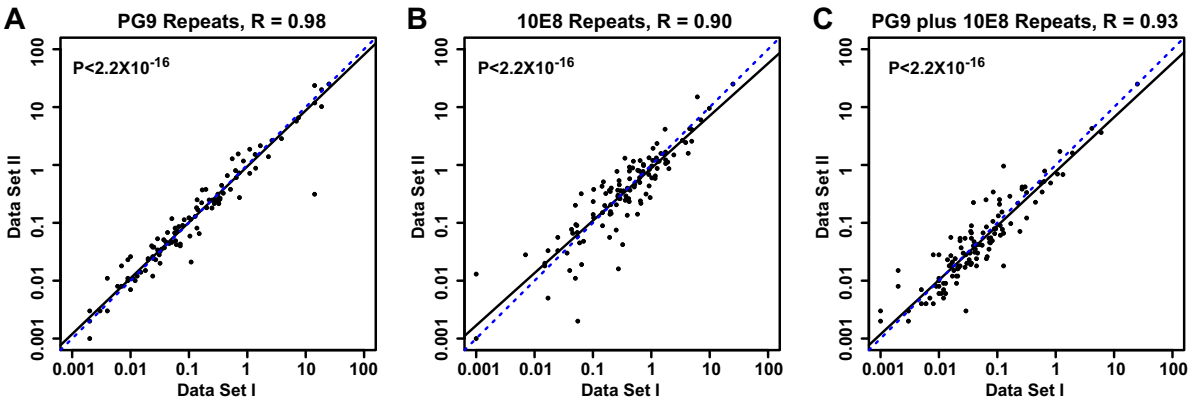

FIG 2 Correlations of repeat experimental IC_{50} data. The single MAbs PG9 (A) and 10E8 (B) and a mixture of the two (C) were assessed independently in set I and set II experiments. The repeat IC_{50} titers on 125 HIV-1 Env-pseudotyped strains are shown on the *x* axis (set I) and *y* axis (set II). The blue dashed lines show the ideal identical IC_{50}s from both data sets, while the black solid lines show the best fit of the experimental data. Pearson correlation *P* values were less than 2.2×10^{-16} in all three cases. Pearson correlation coefficient *R* value are shown.

P-B curves to the theoretical curves for individual MAbs and combinations of MAbs. In all cases, the experimental curves of MAb combinations shifted to the left compared to the corresponding single-MAb curves, indicating improved neutralization breadth at most IC_{50}s (Fig. 3A and B). In addition, increasing virus coverage was also observed with double-, triple-, and quadruple-MAb combinations (Fig. 3C). For example, at the IC_{50} cutoff of 1 μg/ml, the CD4bs MAbs VRC07 and 3BNC117 neutralized 83% and 79% of the viruses, respectively, representing the best coverage by single MAbs (Fig. 4). In contrast, all double combinations neutralized 89 to 98% of the viruses at this cutoff concentration, and all triple and quadruple combinations neutralized 98 to 100% of the viruses. Notably, this virus coverage was retained at relatively low MAb concentrations, i.e., at an IC_{50} cutoff of 1 μg/ml. Similar virus coverage improvement for MAb combinations was observed using IC_{80} rather than IC_{50} cutoff values (Fig. 4).

Complementary neutralization profiles of single MAbs contributed to improved neutralization breadth. To further understand the observed neutralization breadths of MAb combinations, heat maps were generated to illustrate the neutralizing activities of MAbs and their combinations against individual virus strains (Fig. 5). These heat maps produced three main observations. First, the patterns of sensitivity and resistance for similar MAbs and MAb combinations were similar between the two data sets. For example, the pattern for the double combination VRC07 and PGT128 was similar to that of 3BNC117 and 10-1074. Only 1 out of 125 virus strains was resistant to all four set I MAbs, while all 125 strains were neutralized by at least one of the set II MAbs (Fig. 5). Second, when antibodies were combined, a positive antibody in the mixture enabled neutralization of strains that were resistant to the negative antibody in the mixture. Consequently, the MAb combinations neutralized all virus strains that were sensitive to at least one component MAb, and virus strains that were not neutralized by MAb combinations were resistant to all corresponding component MAbs when tested individually. For example, the V3-glycan MAbs 10-1074 and PGT128 lacked neutralization against about 40% of the viral strains, but these strains were often potently neutralized by MAbs to other epitopes. Third, when three or four MAbs were combined, nearly full virus coverage was reached, even at the more stringent IC_{80} cutoff, as shown by the higher intensity of red hues for the 3- and 4-MAb combinations (Fig. 4 and 5).

Of note, the combination PG9-PGT128 showed weak neutralization against a few additional virus strains that showed no detectable neutralization by either PG9 or PGT128 individually at 25 μg/ml (Fig. 5A). These strains include 6952.v1.c20, T251-18, and ZM135.10a. Similarly, neither PG9 nor 10-1074 neutralized 191821.E6.1 individually; however, when tested in combination, weak neutralization was observed. Taken together, these results suggest that the observed virus coverage improvement by MAb combinations was contributed mainly by the complementary neutralization profiles of the individual MAbs but that some favorable antibody interactions may occur.

MAb combinations display stronger effects than predicted by an additive model. Since some MAb combinations showed greater potency and breadth than predicted, i.e., the experimental P-B curves shifted to the left of theoretical predicted P-B curves (Fig. 3A and B), we investigated the potential interactions of MAbs in combinations. First, we studied the effect of an inactive MAb(s) ($IC_{50} > 25$ μg/ml) when combined with an active MAb ($IC_{50} < 25$ μg/ml), i.e., only one MAb in the combination showed detectable neutralization of a virus strain when tested alone. Totals of 205 and 244 examples of this scenario were collected from data sets I and II, respectively. The IC_{50} titers of the MAb combination reproduced the titer of the single active MAb with a high degree of accuracy (Fig. 6) (Pearson's test, *R* values of 0.98 and 0.96 for data sets I and II, respectively), suggesting little effect of the inactive MAbs when mixed with the active MAb.

Next, we studied the interaction between active MAbs. When all MAbs in the combination were active (i.e., the IC_{50} was <25 μg/ml when tested individually), estimates of potency (predicted IC_{50} titer) for the combinations were made based on a simple additive model, using the IC_{50} titer of the individual component MAbs as described in Materials and Methods. In contrast to the "theoretical prediction," which uses the best IC_{50} titer of the individual component MAbs (Fig. 3), the additive prediction takes into account the contributions of all component MAbs. For each MAb combination, we compared the experimentally observed IC_{50} titers to the predicted IC_{50} titers across all viruses that were sensitive to each of the component MAbs (see Fig. S1 in the supplemental material). Three distinctive patterns were observed: (i) additive, (ii) synergy, and (iii) potency-dependent effect (Fig. 7). In the case of an additive interaction (Fig. 7A, VRC07-PGT128),

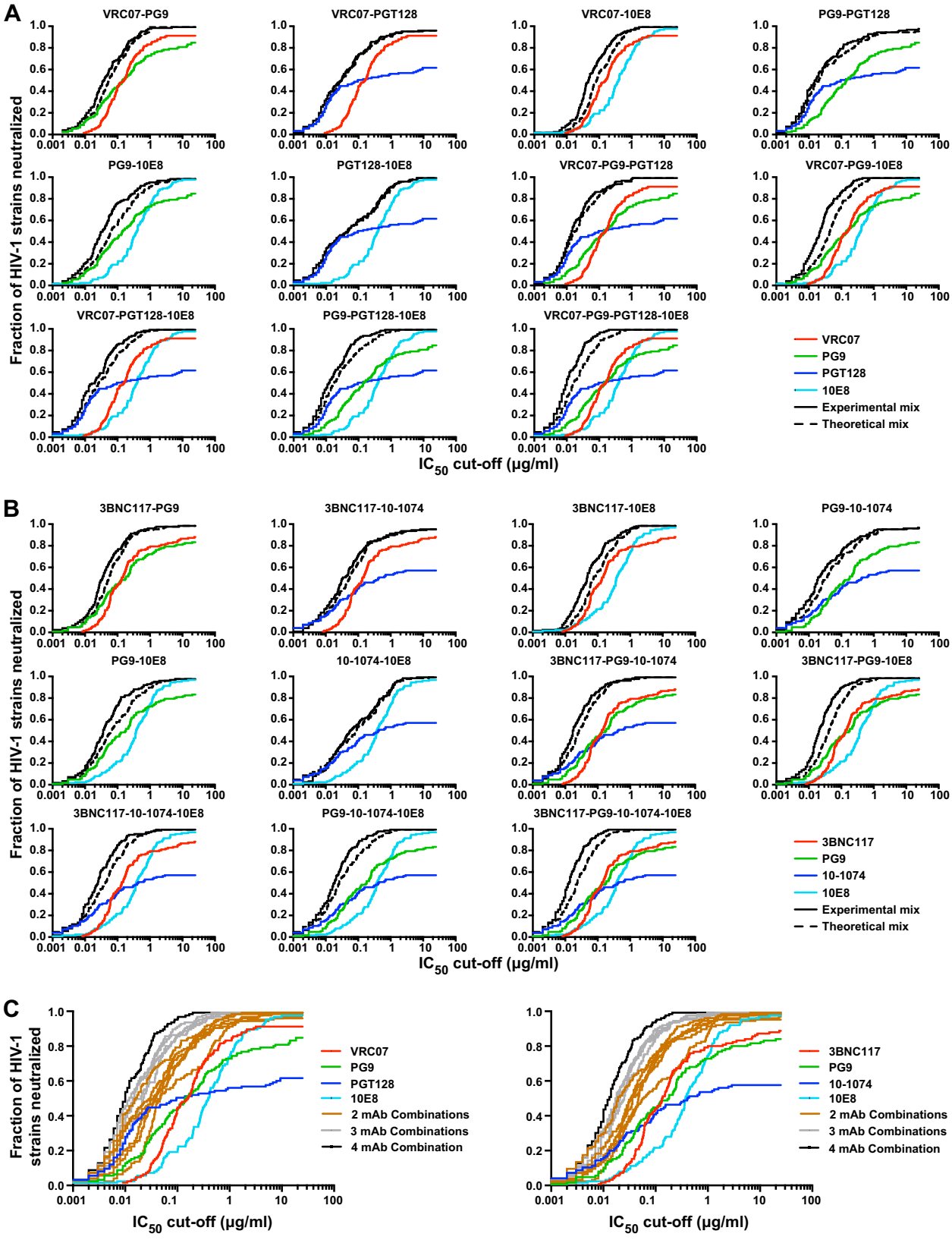

FIG 3 Potency-breadth curves of MAb combinations. A total of 125 HIV-1 strains were tested for neutralization, and the fraction of viruses neutralized is graphed versus the concentration of a single MAb or MAb combination. The P-B curves of MAb combinations are shown according to the concentrations of the single-component antibodies (i.e., all curves start at a maximum antibody concentration of 25 μg/ml). (A) P-B curves of the set I MAbs (VRC07, PG9, PGT128, and 10E8) and their combinations. Each graph shows a combination of two, three, or all four MAbs (solid black lines) and the corresponding single MAbs (colored lines). The theoretical mixture curve of the MAb combination (black dashed lines) is the curve predicted by using the best individual MAb titer as representative of the titer of the MAb combination, while the experimental mixture curve is generated based on the titer of the physical antibody mixture (solid black lines). (B) P-B curves of set II MAbs (3BNC117, PG9, 10-1074, and 10E8). (C) P-B curves of all combinations of set I (left) and set II (right) MAbs. The combinations of two (brown lines), three (gray lines), and all four (black lines) MAbs are shown in the same graph.

A

Number of mAbs			1				2						3				4
VRC07			+				+	+	+				+	+	+		+
PG9				+			+			+	+		+	+		+	+
PGT128					+			+		+		+	+		+	+	+
10E8						+			+		+	+		+	+	+	+
IC50	Virus coverage (%)	0.1 μg/ml	45	44	50	19	69	74	70	79	76	61	86	86	86	91	95
		1 μg/ml	83	73	56	74	98	93	97	93	95	91	98	99	99	99	99
		10 μg/ml	91	81	62	98	99	96	99	96	98	99	99	99	99	99	99
		25 μg/ml	91	85	62	98	99	96	99	98	98	99	99	99	99	99	99
	Median (μg/ml)		0.159	0.142	0.096	0.389	0.038	0.030	0.047	0.016	0.035	0.047	0.014	0.022	0.020	0.012	0.010
	Geometric mean (μg/ml)		0.132	0.104	0.024	0.325	0.043	0.029	0.055	0.023	0.039	0.050	0.018	0.023	0.020	0.015	0.011
IC80	Virus coverage (%)	0.1 μg/ml	14	23	43	2	46	54	24	63	37	45	71	61	58	66	81
		1 μg/ml	72	55	52	23	89	86	86	82	82	63	94	97	93	94	99
		10 μg/ml	90	70	54	91	97	95	99	90	96	97	98	99	99	99	99
		25 μg/ml	91	73	56	97	97	95	99	92	98	99	98	99	99	99	99
	Median (μg/ml)		0.512	0.738	0.652	2.370	0.121	0.089	0.184	0.047	0.186	0.227	0.040	0.076	0.064	0.040	0.029
	Geometric mean (μg/ml)		0.420	0.273	0.060	2.008	0.126	0.094	0.229	0.075	0.191	0.218	0.052	0.080	0.074	0.057	0.038

B

Number of mAbs			1				2						3				4
3BNC117			+				+	+	+				+	+	+		+
PG9				+			+			+	+		+	+		+	+
10-1074					+			+		+		+	+		+	+	+
10E8						+			+		+	+		+	+	+	+
IC50	Virus coverage (%)	0.1 μg/ml	44	45	41	22	76	71	69	74	74	56	86	90	86	87	95
		1 μg/ml	79	73	54	74	97	92	96	94	94	89	98	99	98	100	100
		10 μg/ml	87	82	58	97	99	96	99	97	98	100	100	99	100	100	100
		25 μg/ml	89	84	58	98	99	96	99	98	98	100	100	99	100	100	100
	Median (μg/ml)		0.134	0.180	0.411	0.375	0.034	0.033	0.047	0.019	0.036	0.056	0.017	0.021	0.025	0.018	0.013
	Geometric mean (μg/ml)		0.136	0.098	0.033	0.314	0.038	0.038	0.052	0.026	0.042	0.075	0.020	0.022	0.025	0.019	0.013
IC80	Virus coverage (%)	0.1 μg/ml	14	24	25	2	46	42	28	53	37	30	62	61	51	58	76
		1 μg/ml	66	53	47	25	91	85	83	80	82	65	97	97	94	94	100
		10 μg/ml	81	72	56	92	97	94	99	94	96	99	98	99	100	100	100
		25 μg/ml	83	74	57	96	97	94	99	94	98	100	98	99	100	100	100
	Median (μg/ml)		0.508	0.788	2.740	2.080	0.125	0.138	0.183	0.093	0.189	0.354	0.059	0.083	0.092	0.075	0.051
	Geometric mean (μg/ml)		0.355	0.283	0.172	1.732	0.121	0.154	0.231	0.117	0.187	0.370	0.070	0.081	0.113	0.087	0.051

FIG 4 Percent virus coverage and median and geometric mean IC_{50} and IC_{80} values of set I (A) and set II (B) MAb combinations. The percent virus coverage at the IC_{50} and IC_{80} cutoffs of 0.1, 1, 10, and 50 μg/ml are shown and labeled in red (95 to 100%), orange (90 to 95%), yellow (75 to 90%), green (50 to 75%), and white (0 to 50%). For each MAb or MAb combination, the median value of the entire data set is shown, including resistant viruses, which were assigned a value of 25, while the geometric mean value was calculated for the subset of viruses that were neutralized.

the predicted IC_{50} titers very closely approximated the observed IC_{50} titers for the MAb combination. The average interaction scores, defined as $\log_{10}$ (predicted IC_{50}/observed IC_{50}), were not significantly different from zero (Fig. 8A, gray bars). This indicated that both antibodies were active and contributed to the combined response and that they did not influence each other. The clearest example of this pattern occurred with the double combination of CD4bs and V3-glycan antibodies (VRC07 and PGT128 or 3BNC117 and 10-1074) (Fig. 7A and 8A; see Fig. S1 in the supplemental material).

A second pattern suggested some level of synergy, where the observed IC_{50} titers for the vast majority of virus strains tested were lower than predicted for a given antibody combination (Fig. 7B, PG9-10E8) and the average interaction score was significantly higher than zero (Fig. 8A, blue bars). The cases for synergy involved all double and triple combinations of CD4bs, V1V2-glycan, and MPER antibodies (Fig. 8A; see Fig. S1 in the supplemental material). This observation was consistent in set I and II experiments, even with the replacement of VRC07 with 3BNC117. Of note, this favorable neutralization interaction is subtle and is weaker than that observed for the combination of sCD4 and the CD4i MAb 17b (Fig. 7A). However, given the high level of experimental reproducibility observed between the two data sets for PG9, 10E8, and the PG9-10E8 combination (Fig. 2), and in the cases when one active MAb was mixed with an inactive MAb(s) (Fig. 6), this highly consistent observation suggests that some MAb combinations interact in a manner that is more favorable than predicted by a simple additive model. Interestingly, the interaction scores on the panel of 125 HIV-1 strains showed significant correlations between these combinations (see Fig. S4 in the supplemental material) ($P < 0.019$ using Kendall's Tau rank test) and revealed that a subset of pseudoviruses consistently showed greater than additive potency for all combinations involving 10E8 plus either PG9 or CD4bs antibodies, suggesting an Env-dependent nonstochastic effect for synergy involving 10E8 plus gp120 antibodies. No single genetic subtype of the virus was preferentially represented in the set that was most sensitive to 10E8 enhancement.

The third pattern (potency-dependent effect) showed an apparent transition, which depended on the overall neutralization potency of the MAb combination (Fig. 7C). Here, the most sensitive virus strains showed higher experimental IC_{50}s (lower neutralization potencies) than predicted by the additive model or, in the case of some viruses, less potent than the V3-glycan antibody when used alone (Fig. 7C, data points showing predicted values below the black line of experimental data; see Fig. S1 in the supplemental material), suggesting an inhibition effect. In contrast, the less sensitive virus strains showed experimental IC_{50}s close to or lower than that predicted (Fig. 7C, data points above the black line). Thus, the average behavior across all strains can be additive or even weakly synergistic, yet across the individual strains, there is a potency dependency relationship (Fig. 8A, 3- and 4-MAb

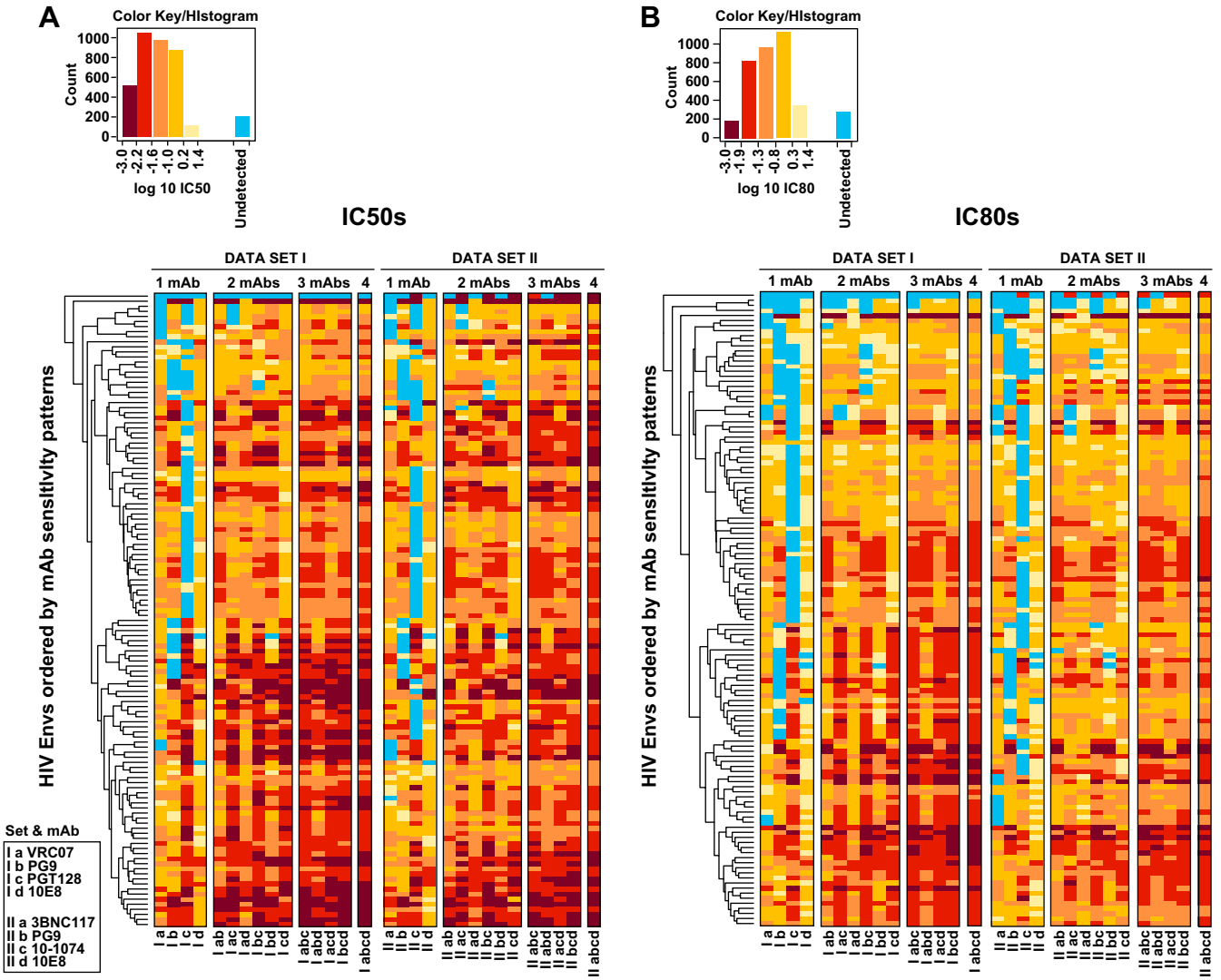

FIG 5 Heat maps displaying IC_{50} and IC_{80} data. Heat maps of IC_{50} data (A) and IC_{80} data (B) were generated as described in Materials and Methods. The potency of the response to a particular Env is indicated in the key (upper left), ranging from weak (light yellow) to very potent (dark red) neutralization. Blue indicates a titer of >25 μg/ml. Antibodies and MAb combinations are arranged in the columns according to the key. The 125 HIV-1 Envs are indicated by rows that are organized according to like patterns of neutralization sensitivity, using hierarchical clustering of the $\log_{10}$ IC_{50} or $\log_{10}$ IC_{80} to aid the eye in resolving patterns.

combinations). This pattern was evident in 11 out of 14 MAb combinations containing the V3-glycan antibody PGT128 or 10-1074, in which the interaction scores for the top 10 sensitive viruses were significantly lower than zero (Fig. 8B and C, red bars; see Fig. S1 in the supplemental material). This observation was further validated by neutralization curves of the PGT128-10E8 and 10-1074–10E8 combinations against the most sensitive viruses (see Fig. S3 and S5 in the supplemental material). Given that the V3 glycan MAbs were generally the main contributors to neutralization of the most highly sensitive viruses, this pattern suggests that the potencies of V3-glycan MAbs were slightly reduced in the presence of other antibodies.

Overall, when predicted IC_{50} titers were compared to the observed IC_{50} titers, less than a 2-fold difference was generally observed for all combinations, i.e., the interaction scores were generally within the range of −0.3 to 0.3 (Fig. 8A), suggesting that the neutralizing activities of MAb combinations were well predicted by the additive model. Subtle but consistent favorable interactions were observed in 15 out of all 22 MAb combinations, including 7 double, 6 triple, and both quadruple combinations (Fig. 8A, blue bars).

DISCUSSION

Prior to 2009, few broadly reactive HIV-1-neutralizing antibodies had been identified, and there was a limited understanding of the major neutralization epitopes on HIV-1 Env. The rapid progress in screening HIV-1-infected donors for serum neutralizing activity (70, 71) and in efficiently isolating HIV-1 MAbs (6) led to the discovery of new highly potent and broadly reactive MAbs (6–10, 14, 15, 25, 26, 37, 41), as well as the structural definition of major sites of neutralization vulnerability on HIV-1 Env (14, 15, 19–22, 24, 26–31, 35, 36, 59–62). In this study, we assessed the *in vitro* neutralizing activities of physical MAb mixtures involving representative broadly neutralizing antibodies targeting four major dis-

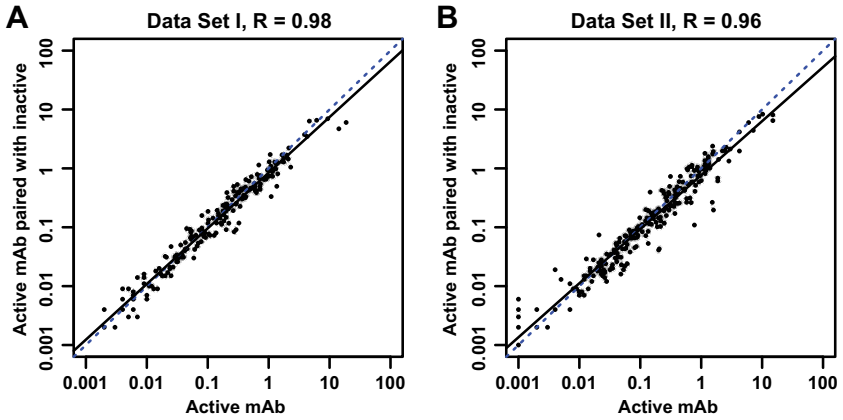

FIG 6 Experimental reproducibility. Shown are the IC_{50}s for a given HIV-1 strain when a MAb that had neutralizing activity was tested by itself (*x* axes) versus when the active MAb was tested in combination with an antibody that had no detectable neutralizing activity against that particular virus (*y* axes). The graphs include all points for which these circumstances arose in data set I (A) or data set II (B). The blue dashed lines show the expected result if there was no difference between the two measures, while the black solid lines show the best fit of the experimental data. The *R* value is the linear correlation coefficient. The very high values of *R* and relatively even narrow scatter about the line are indicative of a high degree of experimental reproducibility between reactions.

tinct epitopes on the HIV-1 Env trimer spike (CD4bs, V1V2-glycan, V3-glycan, and MPER). Neutralization was assessed on a panel of 125 HIV-1 Env-pseudotyped strains representing the major circulating HIV-1 clades. Our results show that MAbs targeting independent sites on HIV-1 Env act in a complementary manner, providing increased neutralization breadth and potency compared to individual MAbs. Double-MAb combinations provided coverage against more than 89% of the viruses tested, and the coverage of triple and quadruple combinations was more than 98%. Notably, this breadth of reactivity could be achieved at IC_{50} levels as low as 1 μg/ml. In most cases, the potency of MAb combinations could be predicted by a model of independent additivity, though in some cases, there were small but statistically significant nonadditive interactions.

We analyzed the MAb interactions by comparing the observed neutralization IC_{50} titers to IC_{50} titers predicted by the additive model. Overall, the neutralization interaction of MAb combination could be closely predicted by an additive model (Fig. 8), suggesting little detrimental impact among MAbs administered together. These results are consistent with our understanding of these four distinct MAb epitopes on the native Env trimer, as shown by various crystal structures (14, 15, 19–22, 24, 26–31, 35, 36, 59–61) and by *in vitro* binding data showing little cross-competition between these MAbs (26, 41). We did observe statistically

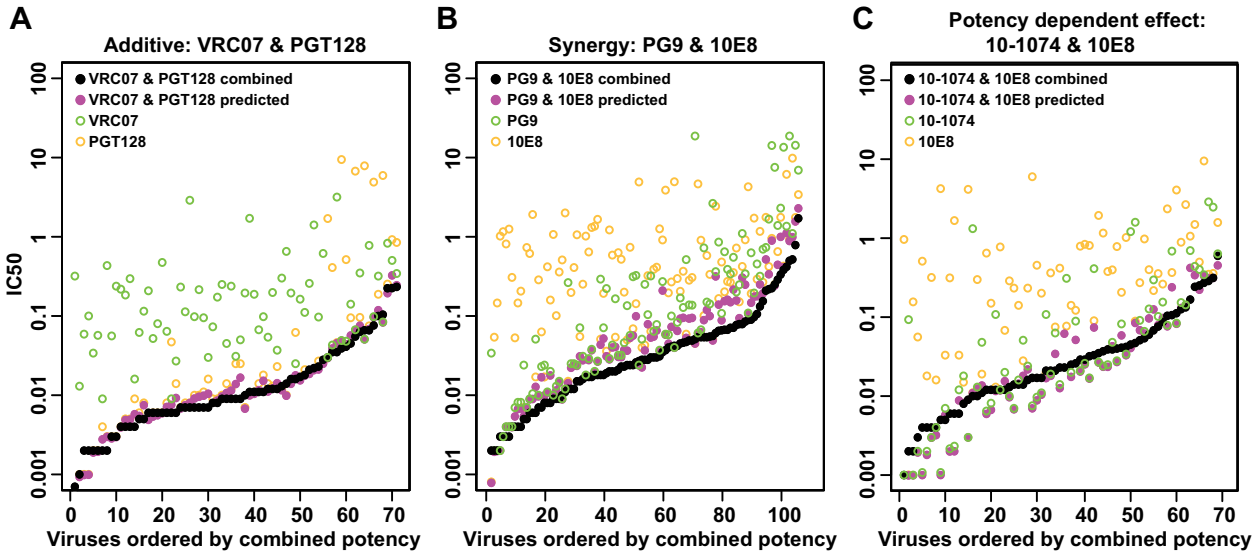

FIG 7 Three patterns of MAb combination effects. (A) The VRC07-PGT128 combination as an example of an additive effect. (B) The PG9-10E8 combination as an example of synergy. (C) The 10-1074–10E8 combination as an example of a potency-dependent effect. For each combination, only viruses that are sensitive to each single component MAb are shown. The viruses are ordered from left to right according to their neutralization sensitivities. For each virus, the IC_{50}s of the single MAbs are shown as green and yellow open circles, while the predicted IC_{50}s of the combinations based on an additive effect are shown as solid magenta dots and the experimental IC_{50}s of the combinations are shown as solid black dots. Synergy is indicated when a black dot is below a magenta dot. Inhibition is shown when a black dot is above a magenta dot.

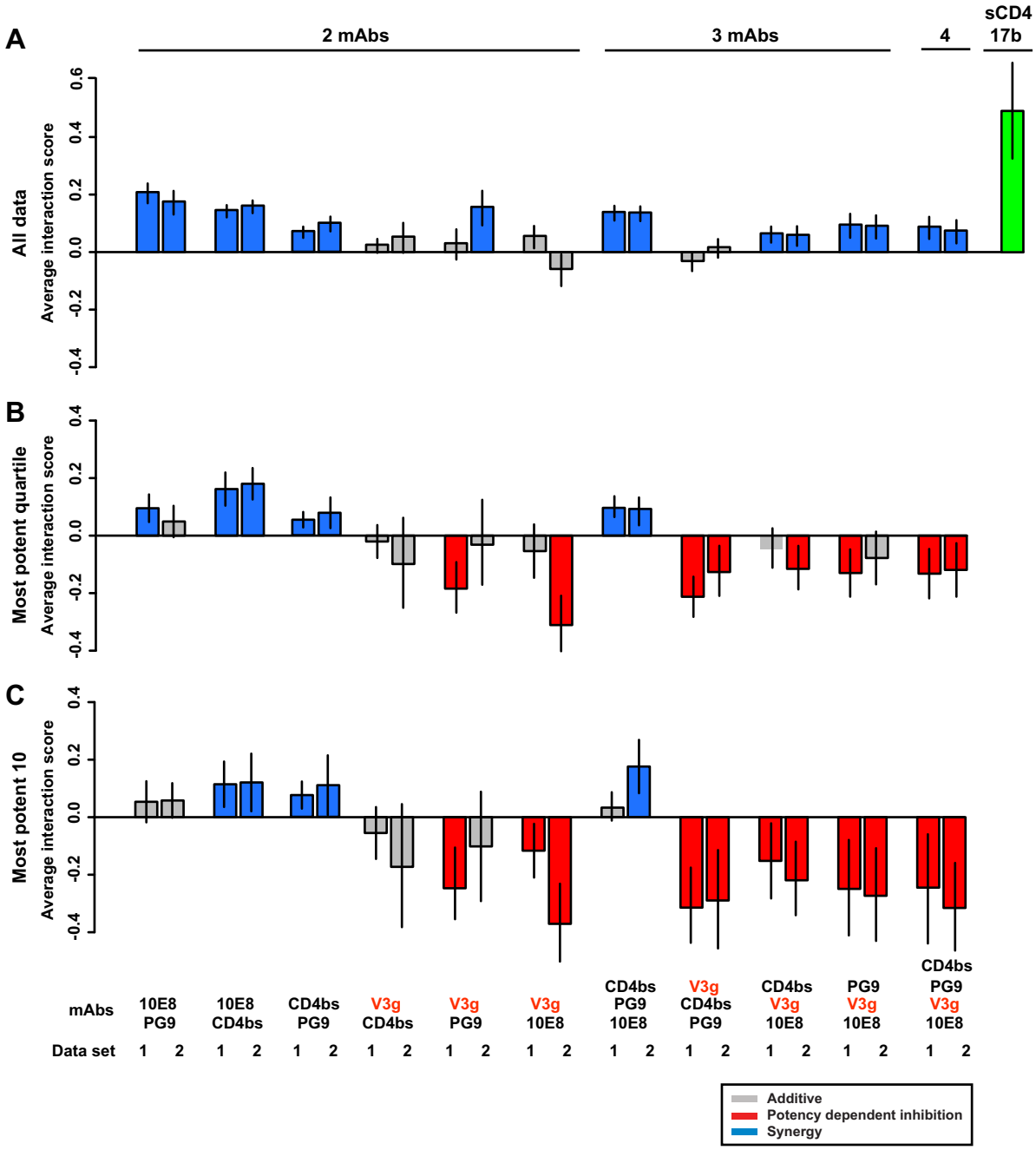

FIG 8 Interaction scores of MAb combinations. For any given MAb combination and virus pair, when each component MAb in the combination neutralized the virus individually, the IC_{50} of the MAb combination was predicted according to the additive model. An interaction score was defined as follows: $\log_{10}$ (predicted IC_{50}/observed IC_{50}). Thus, a positive score indicates that the interaction is more potent than predicted, while a negative score indicates that the interaction is less potent than predicted. (A) The mean interaction scores of each MAb combination for all qualified viruses are shown as the height of the bar, and the error bars reflect the 95% CI of the mean. Blue indicates an average positive interaction score across all viruses included for the specified MAb combination. Similarly, red indicates a negative score and gray indicates that the average score is not significantly different from that predicted. The component MAbs for each combination are shown at the bottom, using CD4bs for VRC07 (data set I) and 3BC117 (data set II) and V3g for PGT128 (data set I) and 10-1074 (data set II). (B) Mean interaction scores on the most potent quartile viruses. (C) Mean interaction scores on the 10 most potent viruses.

significant synergy in 15 out of 22 MAb combinations (Fig. 7 and 8; see Fig. S1 in the supplemental material). This effect was small and generally less than 2-fold different than predicted. However, because of the greatly improved neutralization breadth (~60 to 100%) of recently isolated MAbs, we were able to assess the MAb interactions on a larger panel of viruses. Given the high experimental reproducibility, this subtle but statistically consistent effect was confirmed. The finding of weak synergy is similar to earlier reports, when three reagents (HIVIG, 2F5, and 2G12) were mixed and tested on 15 HIV-1 isolates (72) and when 4 MAbs (b12, 2G12, 2F5, and 4E10) were tested on 4 viruses using multiple approaches to assess MAb interactions (73). In a few cases, mainly

occurring for viruses highly sensitive to the V3-glycan MAbs PGT128 and 10-1074, small but consistent unfavorable interactions were noted, suggesting that the less potent MAb within the combination was interfering slightly with the neutralization activity of the V3-glycan MAb.

Overall, our data on the improvement of neutralization potency and breadth by MAb combinations is consistent with several previous reports that generally tested smaller panels of MAbs and viruses (63, 64, 72–75). Due to the recent availability of several of the MAbs tested, our study is the most comprehensive to test double, triple, and quadruple combinations of potent representatives from four major neutralization sites on HIV-1 Env. Based on our data, it is possible to calculate the overall breadth (coverage) of various MAb combinations at various IC_{50} or IC_{80} values (Fig. 4). In addition, the median IC_{50} and IC_{80} values (calculated based on all 125 viruses) and the geometric mean IC_{50} and IC_{80} values (based on the subset of viruses neutralized for any given MAb or MAb combination) provide a means to assess antibody potency. Since both breadth and potency may be important antibody characteristics, we chose not to rank order the antibody combinations within each group of double or triple combinations based on any one value. In addition, the median IC_{50}s for all double combinations were within a 3.5-fold range. For triple combinations, the values were less than 2-fold different. However, there is a clear hierarchy, so that MAb breadth improves with combinations of two, three, or four MAbs. The potencies of MAb combinations also increase, but it is important to note that since our intent was to highlight the potential activity of more than one MAb used together, we calculated IC_{50} and IC_{80} values based on the concentration of each individual MAb in the combination.

Recent *in vivo* studies, in both HIV-1-infected humanized mice and SHIV-infected monkeys, have shown that MAb combinations provide a greater virologic effect than single MAbs (49, 57, 58). These studies also suggested that the *in vivo* effect was at least partially explained by the *in vitro* neutralization potency of the MAbs. HIV-1-specific MAbs have also been shown to provide complete protection against acquisition of SHIV infection. In most of these studies, a single MAb has been shown to afford robust protection, as long as the antibody displayed *in vitro* neutralizing activity against the challenge virus (37, 44–46, 48–50, 76, 77). Several studies demonstrated that weakly neutralizing or nonneutralizing antibodies provided little protection against infection (45, 78–80). Similarly, a number of studies have shown a general correlation between the level of *in vitro* neutralization and the level of protection (37, 44, 48, 77, 79, 81), although Fc-mediated effector functions also likely play a role (82) and some antibodies appear to provide *in vivo* protection that is greater than predicted by *in vitro* neutralization titers (80). We also recently demonstrated that improved *in vitro* neutralization of a MAb predicted a lower plasma concentration required for effective protection (37). Overall, the *in vivo* efficacy of MAbs against HIV-1 in humans may depend on the neutralization potency, breadth of virus coverage, Fc-mediated effector functions, and other characteristics, including pharmacokinetic properties and the presence of antibody at sites of infection (1, 4). Since *in vitro* neutralization breadth and potency are likely critical parameters, our data here can inform the choice of potentially effective MAb combinations.

In summary, we observed substantially improved *in vitro* neutralization potency and breadth by combining broadly reactive MAbs targeting distinct epitopes, including CD4bs, V1V2-glycan, V3-glycan, and MPER. Such improvement was closely predicted by an additive model and explained by complementary neutralization profiles of component MAbs. There was no substantial negative impact when these MAbs were used in combination. Overall, these data provide a rationale for obtaining increased antibody potency and breadth of coverage *in vivo* with antibody-based combinations for the treatment or prevention of HIV-1 infection.

ACKNOWLEDGMENTS

We thank Peggy Johnston, Alan Lapedes, James Theiler, and Tanmoy Bhattacharya for helpful discussions and advice. We thank Ellen Turk and Chien-Li Lin for their technical assistance with the performance of the automated viral neutralization assays.

This work was funded by the intramural research program of the Vaccine Research Center, NIAID, NIH, and by a grant from the Bill and Melinda Gates Foundation (Collaboration for AIDS Vaccine Discovery; no. 1032144). B.K. and K.W. were also partially supported in this work through a Center for HIV/AIDS Vaccine Immunology-Immunogen Discovery grant (CHAVI-ID; UM1 AI100645).

REFERENCES

1. **Mascola JR, Montefiori DC.** 2010. The role of antibodies in HIV vaccines. Annu Rev Immunol **28:**413–444. http://dx.doi.org/10.1146/annurev-immunol-030409-101256.
2. **Burton DR, Poignard P, Stanfield RL, Wilson IA.** 2012. Broadly neutralizing antibodies present new prospects to counter highly antigenically diverse viruses. Science **337:**183–186. http://dx.doi.org/10.1126/science.1225416.
3. **Kwong PD, Mascola JR.** 2012. Human antibodies that neutralize HIV-1: identification, structures, and B cell ontogenies. Immunity **37:**412–425. http://dx.doi.org/10.1016/j.immuni.2012.08.012.
4. **Klein F, Mouquet H, Dosenovic P, Scheid JF, Scharf L, Nussenzweig MC.** 2013. Antibodies in HIV-1 vaccine development and therapy. Science **341:**1199–1204. http://dx.doi.org/10.1126/science.1241144.
5. **Kwong PD, Mascola JR, Nabel GJ.** 2013. Broadly neutralizing antibodies and the search for an HIV-1 vaccine: the end of the beginning. Nat Rev Immunol **13:**693–701. http://dx.doi.org/10.1038/nri3516.
6. **Scheid JF, Mouquet H, Feldhahn N, Seaman MS, Velinzon K, Pietzsch J, Ott RG, Anthony RM, Zebroski H, Hurley A, Phogat A, Chakrabarti B, Li Y, Connors M, Pereyra F, Walker BD, Wardemann H, Ho D, Wyatt RT, Mascola JR, Ravetch JV, Nussenzweig MC.** 2009. Broad diversity of neutralizing antibodies isolated from memory B cells in HIV-infected individuals. Nature **458:**636–640. http://dx.doi.org/10.1038/nature07930.
7. **Wu X, Yang ZY, Li Y, Hogerkorp CM, Schief WR, Seaman MS, Zhou T, Schmidt SD, Wu L, Xu L, Longo NS, McKee K, O'Dell S, Louder MK, Wycuff DL, Feng Y, Nason M, Doria-Rose N, Connors M, Kwong PD, Roederer M, Wyatt RT, Nabel GJ, Mascola JR.** 2010. Rational design of envelope identifies broadly neutralizing human monoclonal antibodies to HIV-1. Science **329:**856–861. http://dx.doi.org/10.1126/science.1187659.
8. **Walker LM, Phogat SK, Chan-Hui PY, Wagner D, Phung P, Goss JL, Wrin T, Simek MD, Fling S, Mitcham JL, Lehrman JK, Priddy FH, Olsen OA, Frey SM, Hammond PW, Protocol G, Principal Investigators, Kaminsky S, Zamb T, Moyle M, Koff WC, Poignard P, Burton DR.** 2009. Broad and potent neutralizing antibodies from an African donor reveal a new HIV-1 vaccine target. Science **326:**285–289. http://dx.doi.org/10.1126/science.1178746.
9. **Walker LM, Huber M, Doores KJ, Falkowska E, Pejchal R, Julien JP, Wang SK, Ramos A, Chan-Hui PY, Moyle M, Mitcham JL, Hammond PW, Olsen OA, Phung P, Fling S, Wong CH, Phogat S, Wrin T, Simek MD, Protocol G, Principal Investigators, Koff WC, Wilson IA, Burton DR, Poignard P.** 2011. Broad neutralization coverage of HIV by multiple highly potent antibodies. Nature **477:**466–470. http://dx.doi.org/10.1038/nature10373.
10. **Huang J, Ofek G, Laub L, Louder MK, Doria-Rose NA, Longo NS, Imamichi H, Bailer RT, Chakrabarti B, Sharma SK, Alam SM, Wang T, Yang Y, Zhang B, Migueles SA, Wyatt R, Haynes BF, Kwong PD, Mascola JR, Connors M.** 2012. Broad and potent neutralization of HIV-1

by a gp41-specific human antibody. Nature **491:**406–412. http://dx.doi.org/10.1038/nature11544.

11. **Corti D, Langedijk JP, Hinz A, Seaman MS, Vanzetta F, Fernandez-Rodriguez BM, Silacci C, Pinna D, Jarrossay D, Balla-Jhagjhoorsingh S, Willems B, Zekveld MJ, Dreja H, O'Sullivan E, Pade C, Orkin C, Jeffs SA, Montefiori DC, Davis D, Weissenhorn W, McKnight A, Heeney JL, Sallusto F, Sattentau QJ, Weiss RA, Lanzavecchia A.** 2010. Analysis of memory B cell responses and isolation of novel monoclonal antibodies with neutralizing breadth from HIV-1-infected individuals. PLoS One **5:**e8805. http://dx.doi.org/10.1371/journal.pone.0008805.
12. **Wardemann H, Yurasov S, Schaefer A, Young JW, Meffre E, Nussenzweig MC.** 2003. Predominant autoantibody production by early human B cell precursors. Science **301:**1374–1377. http://dx.doi.org/10.1126/science.1086907.
13. **Tiller T, Meffre E, Yurasov S, Tsuiji M, Nussenzweig MC, Wardemann H.** 2008. Efficient generation of monoclonal antibodies from single human B cells by single cell RT-PCR and expression vector cloning. J Immunol Methods **329:**112–124. http://dx.doi.org/10.1016/j.jim.2007.09.017.
14. **Mouquet H, Scharf L, Euler Z, Liu Y, Eden C, Scheid JF, Halper-Stromberg A, Gnanapragasam PN, Spencer DI, Seaman MS, Schuitemaker H, Feizi T, Nussenzweig MC, Bjorkman PJ.** 2012. Complex-type N-glycan recognition by potent broadly neutralizing HIV antibodies. Proc Natl Acad Sci U S A **109:**E3268–E3277. http://dx.doi.org/10.1073/pnas.1217207109.
15. **Scheid JF, Mouquet H, Ueberheide B, Diskin R, Klein F, Oliveira TY, Pietzsch J, Fenyo D, Abadir A, Velinzon K, Hurley A, Myung S, Boulad F, Poignard P, Burton DR, Pereyra F, Ho DD, Walker BD, Seaman MS, Bjorkman PJ, Chait BT, Nussenzweig MC.** 2011. Sequence and structural convergence of broad and potent HIV antibodies that mimic CD4 binding. Science **333:**1633–1637. http://dx.doi.org/10.1126/science.1207227.
16. **Burton DR, Pyati J, Koduri R, Sharp SJ, Thornton GB, Parren PW, Sawyer LS, Hendry RM, Dunlop N, Nara PL, Lamacchia M, Garratty E, Stiehm ER, Bryson YJ, Cao Y, Moore JP, Ho DD, Barbas CF.** 1994. Efficient neutralization of primary isolates of HIV-1 by a recombinant human monoclonal antibody. Science **266:**1024–1027. http://dx.doi.org/10.1126/science.7973652.
17. **Liao HX, Lynch R, Zhou T, Gao F, Alam SM, Boyd SD, Fire AZ, Roskin KM, Schramm CA, Zhang Z, Zhu J, Shapiro L, NISC Comparative Sequencing Program, Mullikin JC, Gnanakaran S, Hraber P, Wiehe K, Kelsoe G, Yang G, Xia SM, Montefiori DC, Parks R, Lloyd KE, Scearce RM, Soderberg KA, Cohen M, Kamanga G, Louder MK, Tran LM, Chen Y, Cai F, Chen S, Moquin S, Du X, Joyce MG, Srivatsan S, Zhang B, Zheng A, Shaw GM, Hahn BH, Kepler TB, Korber BT, Kwong PD, Mascola JR, Haynes BF.** 2013. Co-evolution of a broadly neutralizing HIV-1 antibody and founder virus. Nature **496:**469–476. http://dx.doi.org/10.1038/nature12053.
18. **Wu X, Zhou T, Zhu J, Zhang B, Georgiev I, Wang C, Chen X, Longo NS, Louder M, McKee K, O'Dell S, Perfetto S, Schmidt SD, Shi W, Wu L, Yang Y, Yang ZY, Yang Z, Zhang Z, Bonsignori M, Crump JA, Kapiga SH, Sam NE, Haynes BF, Simek M, Burton DR, Koff WC, Doria-Rose NA, Connors M, NISC Comparative Sequencing Program, Mullikin JC, Nabel GJ, Roederer M, Shapiro L, Kwong PD, Mascola JR.** 2011. Focused evolution of HIV-1 neutralizing antibodies revealed by structures and deep sequencing. Science **333:**1593–1602. http://dx.doi.org/10.1126/science.1207532.
19. **Zhou T, Georgiev I, Wu X, Yang ZY, Dai K, Finzi A, Kwon YD, Scheid JF, Shi W, Xu L, Yang Y, Zhu J, Nussenzweig MC, Sodroski J, Shapiro L, Nabel GJ, Mascola JR, Kwong PD.** 2010. Structural basis for broad and potent neutralization of HIV-1 by antibody VRC01. Science **329:**811–817. http://dx.doi.org/10.1126/science.1192819.
20. **Zhou T, Xu L, Dey B, Hessell AJ, Van Ryk D, Xiang SH, Yang X, Zhang MY, Zwick MB, Arthos J, Burton DR, Dimitrov DS, Sodroski J, Wyatt R, Nabel GJ, Kwong PD.** 2007. Structural definition of a conserved neutralization epitope on HIV-1 gp120. Nature **445:**732–737. http://dx.doi.org/10.1038/nature05580.
21. **Zhou T, Zhu J, Wu X, Moquin S, Zhang B, Acharya P, Georgiev IS, Altae-Tran HR, Chuang GY, Joyce MG, Do Kwon Y, Longo NS, Louder MK, Luongo T, McKee K, Schramm CA, Skinner J, Yang Y, Yang Z, Zhang Z, Zheng A, Bonsignori M, Haynes BF, Scheid JF, Nussenzweig MC, Simek M, Burton DR, Koff WC, NISC Comparative Sequencing Program, Mullikin JC, Connors M, Shapiro L, Nabel GJ, Mascola JR, Kwong PD.** 2013. Multidonor analysis reveals structural elements, genetic determinants, and maturation pathway for HIV-1 neutralization by VRC01-class antibodies. Immunity **39:**245–258. http://dx.doi.org/10.1016/j.immuni.2013.04.012.
22. **Julien JP, Sok D, Khayat R, Lee JH, Doores KJ, Walker LM, Ramos A, Diwanji DC, Pejchal R, Cupo A, Katpally U, Depetris RS, Stanfield RL, McBride R, Marozsan AJ, Paulson JC, Sanders RW, Moore JP, Burton DR, Poignard P, Ward AB, Wilson IA.** 2013. Broadly neutralizing antibody PGT121 allosterically modulates CD4 binding via recognition of the HIV-1 gp120 V3 base and multiple surrounding glycans. PLoS Pathog **9:**e1003342. http://dx.doi.org/10.1371/journal.ppat.1003342.
23. **Kong L, Lee JH, Doores KJ, Murin CD, Julien JP, McBride R, Liu Y, Marozsan A, Cupo A, Klasse PJ, Hoffenberg S, Caulfield M, King CR, Hua Y, Le KM, Khayat R, Deller MC, Clayton T, Tien H, Feizi T, Sanders RW, Paulson JC, Moore JP, Stanfield RL, Burton DR, Ward AB, Wilson IA.** 2013. Supersite of immune vulnerability on the glycosylated face of HIV-1 envelope glycoprotein gp120. Nat Struct Mol Biol **20:**796–803. http://dx.doi.org/10.1038/nsmb.2594.
24. **Pejchal R, Doores KJ, Walker LM, Khayat R, Huang PS, Wang SK, Stanfield RL, Julien JP, Ramos A, Crispin M, Depetris R, Katpally U, Marozsan A, Cupo A, Maloveste S, Liu Y, McBride R, Ito Y, Sanders RW, Ogohara C, Paulson JC, Feizi T, Scanlan CN, Wong CH, Moore JP, Olson WC, Ward AB, Poignard P, Schief WR, Burton DR, Wilson IA.** 2011. A potent and broad neutralizing antibody recognizes and penetrates the HIV glycan shield. Science **334:**1097–1103. http://dx.doi.org/10.1126/science.1213256.
25. **Sok D, Doores KJ, Briney B, Le KM, Saye-Francisco KL, Ramos A, Kulp DW, Julien JP, Menis S, Wickramasinghe L, Seaman MS, Schief WR, Wilson IA, Poignard P, Burton DR.** 2014. Promiscuous glycan site recognition by antibodies to the high-mannose patch of gp120 broadens neutralization of HIV. Sci Transl Med **6:**236ra263. http://dx.doi.org/10.1126/scitranslmed.3008104.
26. **Doria-Rose NA, Schramm CA, Gorman J, Moore PL, Bhiman JN, DeKosky BJ, Ernandes MJ, Georgiev IS, Kim HJ, Pancera M, Staupe RP, Altae-Tran HR, Bailer RT, Crooks ET, Cupo A, Druz A, Garrett NJ, Hoi KH, Kong R, Louder MK, Longo NS, McKee K, Nonyane M, O'Dell S, Roark RS, Rudicell RS, Schmidt SD, Sheward DJ, Soto C, Wibmer CK, Yang Y, Zhang Z, NISC Comparative Sequencing Program, Mullikin JC, Binley JM, Sanders RW, Wilson IA, Moore JP, Ward AB, Georgiou G, Williamson C, Abdool Karim SS, Morris L, Kwong PD, Shapiro L, Mascola JR.** 2014. Developmental pathway for potent V1V2-directed HIV-neutralizing antibodies. Nature **509:**55–62. http://dx.doi.org/10.1038/nature13036.
27. **Julien JP, Lee JH, Cupo A, Murin CD, Derking R, Hoffenberg S, Caulfield MJ, King CR, Marozsan AJ, Klasse PJ, Sanders RW, Moore JP, Wilson IA, Ward AB.** 2013. Asymmetric recognition of the HIV-1 trimer by broadly neutralizing antibody PG9. Proc Natl Acad Sci U S A **110:**4351–4356. http://dx.doi.org/10.1073/pnas.1217537110.
28. **McLellan JS, Pancera M, Carrico C, Gorman J, Julien JP, Khayat R, Louder R, Pejchal R, Sastry M, Dai K, O'Dell S, Patel N, Shahzad-ul Hussan S, Yang Y, Zhang B, Zhou T, Zhu J, Boyington JC, Chuang GY, Diwanji D, Georgiev I, Kwon YD, Lee D, Louder MK, Moquin S, Schmidt SD, Yang ZY, Bonsignori M, Crump JA, Kapiga SH, Sam NE, Haynes BF, Burton DR, Koff WC, Walker LM, Phogat S, Wyatt R, Orwenyo J, Wang LX, Arthos J, Bewley CA, Mascola JR, Nabel GJ, Schief WR, Ward AB, Wilson IA, Kwong PD.** 2011. Structure of HIV-1 gp120 V1/V2 domain with broadly neutralizing antibody PG9. Nature **480:**336–343. http://dx.doi.org/10.1038/nature10696.
29. **Pancera M, McLellan JS, Wu X, Zhu J, Changela A, Schmidt SD, Yang Y, Zhou T, Phogat S, Mascola JR, Kwong PD.** 2010. Crystal structure of PG16 and chimeric dissection with somatically related PG9: structure-function analysis of two quaternary-specific antibodies that effectively neutralize HIV-1. J Virol **84:**8098–8110. http://dx.doi.org/10.1128/JVI.00966-10.
30. **Pancera M, Shahzad-Ul-Hussan S, Doria-Rose NA, McLellan JS, Bailer RT, Dai K, Loesgen S, Louder MK, Staupe RP, Yang Y, Zhang B, Parks R, Eudailey J, Lloyd KE, Blinn J, Alam SM, Haynes BF, Amin MN, Wang LX, Burton DR, Koff WC, Nabel GJ, Mascola JR, Bewley CA, Kwong PD.** 2013. Structural basis for diverse N-glycan recognition by HIV-1-neutralizing V1-V2-directed antibody PG16. Nat Struct Mol Biol **20:**804–813. http://dx.doi.org/10.1038/nsmb.2600.
31. **Pejchal R, Walker LM, Stanfield RL, Phogat SK, Koff WC, Poignard P, Burton DR, Wilson IA.** 2010. Structure and function of broadly reactive antibody PG16 reveal an H3 subdomain that mediates potent neutraliza-

tion of HIV-1. Proc Natl Acad Sci U S A **107:**11483–11488. http://dx.doi.org/10.1073/pnas.1004600107.
32. **Muster T, Steindl F, Purtscher M, Trkola A, Klima A, Himmler G, Ruker F, Katinger H.** 1993. A conserved neutralizing epitope on gp41 of human immunodeficiency virus type 1. J Virol **67:**6642–6647.
33. **Trkola A, Pomales AB, Yuan H, Korber B, Maddon PJ, Allaway GP, Katinger H, Barbas CF, III, Burton DR, Ho DD.** 1995. Cross-clade neutralization of primary isolates of human immunodeficiency virus type 1 by human monoclonal antibodies and tetrameric CD4-IgG. J Virol **69:**6609–6617.
34. **Zwick MB, Labrijn AF, Wang M, Spenlehauer C, Saphire EO, Binley JM, Moore JP, Stiegler G, Katinger H, Burton DR, Parren PW.** 2001. Broadly neutralizing antibodies targeted to the membrane-proximal external region of human immunodeficiency virus type 1 glycoprotein gp41. J Virol **75:**10892–10905. http://dx.doi.org/10.1128/JVI.75.22.10892-10905.2001.
35. **Ofek G, Tang M, Sambor A, Katinger H, Mascola JR, Wyatt R, Kwong PD.** 2004. Structure and mechanistic analysis of the anti-human immunodeficiency virus type 1 antibody 2F5 in complex with its gp41 epitope. J Virol **78:**10724–10737. http://dx.doi.org/10.1128/JVI.78.19.10724-10737.2004.
36. **Cardoso RM, Zwick MB, Stanfield RL, Kunert R, Binley JM, Katinger H, Burton DR, Wilson IA.** 2005. Broadly neutralizing anti-HIV antibody 4E10 recognizes a helical conformation of a highly conserved fusion-associated motif in gp41. Immunity **22:**163–173. http://dx.doi.org/10.1016/j.immuni.2004.12.011.
37. **Rudicell RS, Kwon YD, Ko SY, Pegu A, Louder MK, Georgiev IS, Wu X, Zhu J, Boyington JC, Chen X, Shi W, Yang ZY, Doria-Rose NA, McKee K, O'Dell S, Schmidt SD, Chuang GY, Druz A, Soto C, Yang Y, Zhang B, Zhou T, Todd JP, Lloyd KE, Eudailey J, Roberts KE, Donald BR, Bailer RT, Ledgerwood J, NISC Comparative Sequencing Program, Mullikin JC, Shapiro L, Koup RA, Graham BS, Nason MC, Connors M, Haynes BF, Rao SS, Roederer M, Kwong PD, Mascola JR, Nabel GJ.** 2014. Enhanced potency of a broadly neutralizing HIV-1 antibody in vitro improves protection against lentiviral infection in vivo. J Virol **88:**12669–12682. http://dx.doi.org/10.1128/JVI.02213-14.
38. **Scharf L, Scheid JF, Lee JH, West AP, Jr, Chen C, Gao H, Gnanapragasam PN, Mares R, Seaman MS, Ward AB, Nussenzweig MC, Bjorkman PJ.** 2014. Antibody 8ANC195 reveals a site of broad vulnerability on the HIV-1 envelope spike. Cell Rep **7:**785–795. http://dx.doi.org/10.1016/j.celrep.2014.04.001.
39. **Falkowska E, Le KM, Ramos A, Doores KJ, Lee JH, Blattner C, Ramirez A, Derking R, van Gils MJ, Liang CH, McBride R, von Bredow B, Shivatare SS, Wu CY, Chan-Hui PY, Liu Y, Feizi T, Zwick MB, Koff WC, Seaman MS, Swiderek K, Moore JP, Evans D, Paulson JC, Wong CH, Ward AB, Wilson IA, Sanders RW, Poignard P, Burton DR.** 2014. Broadly neutralizing HIV antibodies define a glycan-dependent epitope on the prefusion conformation of gp41 on cleaved envelope trimers. Immunity **40:**657–668. http://dx.doi.org/10.1016/j.immuni.2014.04.009.
40. **Blattner C, Lee JH, Sliepen K, Derking R, Falkowska E, de la Pena AT, Cupo A, Julien JP, van Gils M, Lee PS, Peng W, Paulson JC, Poignard P, Burton DR, Moore JP, Sanders RW, Wilson IA, Ward AB.** 2014. Structural delineation of a quaternary, cleavage-dependent epitope at the gp41-gp120 interface on intact HIV-1 Env trimers. Immunity **40:**669–680. http://dx.doi.org/10.1016/j.immuni.2014.04.008.
41. **Huang J, Kang BH, Pancera M, Lee JH, Tong T, Feng Y, Georgiev IS, Chuang GY, Druz A, Doria-Rose NA, Laub L, Sliepen K, van Gils MJ, de la Pena AT, Derking R, Klasse PJ, Migueles SA, Bailer RT, Alam M, Pugach P, Haynes BF, Wyatt RT, Sanders RW, Binley JM, Ward AB, Mascola JR, Kwong PD, Connors M.** 2014. Broad and potent HIV-1 neutralization by a human antibody that binds the gp41-gp120 interface. Nature **515:**138–142. http://dx.doi.org/10.1038/nature13601.
42. **Haynes BF, Kelsoe G, Harrison SC, Kepler TB.** 2012. B-cell-lineage immunogen design in vaccine development with HIV-1 as a case study. Nat Biotechnol **30:**423–433. http://dx.doi.org/10.1038/nbt.2197.
43. **Mascola JR, Haynes BF.** 2013. HIV-1 neutralizing antibodies: understanding nature's pathways. Immunol Rev **254:**225–244. http://dx.doi.org/10.1111/imr.12075.
44. **Mascola JR, Stiegler G, VanCott TC, Katinger H, Carpenter CB, Hanson CE, Beary H, Hayes D, Frankel SS, Birx DL, Lewis MG.** 2000. Protection of macaques against vaginal transmission of a pathogenic HIV-1/SIV chimeric virus by passive infusion of neutralizing antibodies. Nat Med **6:**207–210. http://dx.doi.org/10.1038/72318.
45. **Parren PW, Marx PA, Hessell AJ, Luckay A, Harouse J, Cheng-Mayer C, Moore JP, Burton DR.** 2001. Antibody protects macaques against vaginal challenge with a pathogenic R5 simian/human immunodeficiency virus at serum levels giving complete neutralization in vitro. J Virol **75:**8340–8347. http://dx.doi.org/10.1128/JVI.75.17.8340-8347.2001.
46. **Hessell AJ, Poignard P, Hunter M, Hangartner L, Tehrani DM, Bleeker WK, Parren PW, Marx PA, Burton DR.** 2009. Effective, low-titer antibody protection against low-dose repeated mucosal SHIV challenge in macaques. Nat Med **15:**951–954. http://dx.doi.org/10.1038/nm.1974.
47. **Johnson PR, Schnepp BC, Zhang J, Connell MJ, Greene SM, Yuste E, Desrosiers RC, Clark KR.** 2009. Vector-mediated gene transfer engenders long-lived neutralizing activity and protection against SIV infection in monkeys. Nat Med **15:**901–906. http://dx.doi.org/10.1038/nm.1967.
48. **Moldt B, Rakasz EG, Schultz N, Chan-Hui PY, Swiderek K, Weisgrau KL, Piaskowski SM, Bergman Z, Watkins DI, Poignard P, Burton DR.** 2012. Highly potent HIV-specific antibody neutralization in vitro translates into effective protection against mucosal SHIV challenge in vivo. Proc Natl Acad Sci U S A **109:**18921–18925. http://dx.doi.org/10.1073/pnas.1214785109.
49. **Shingai M, Nishimura Y, Klein F, Mouquet H, Donau OK, Plishka R, Buckler-White A, Seaman M, Piatak M, Jr, Lifson JD, Dimitrov DS, Nussenzweig MC, Martin MA.** 2013. Antibody-mediated immunotherapy of macaques chronically infected with SHIV suppresses viraemia. Nature **503:**277–280. http://dx.doi.org/10.1038/nature12746.
50. **Pegu A, Yang ZY, Boyington JC, Wu L, Ko SY, Schmidt SD, McKee K, Kong WP, Shi W, Chen X, Todd JP, Letvin NL, Huang J, Nason MC, Hoxie JA, Kwong PD, Connors M, Rao SS, Mascola JR, Nabel GJ.** 2014. Neutralizing antibodies to HIV-1 envelope protect more effectively in vivo than those to the CD4 receptor. Sci Transl Med **6:**243ra88. http://dx.doi.org/10.1126/scitranslmed.3008992.
51. **Balazs AB, Chen J, Hong CM, Rao DS, Yang L, Baltimore D.** 2012. Antibody-based protection against HIV infection by vectored immunoprophylaxis. Nature **481:**81–84. http://dx.doi.org/10.1038/nature10660.
52. **Balazs AB, Ouyang Y, Hong CM, Chen J, Nguyen SM, Rao DS, An DS, Baltimore D.** 2014. Vectored immunoprophylaxis protects humanized mice from mucosal HIV transmission. Nat Med **20:**296–300. http://dx.doi.org/10.1038/nm.3471.
53. **Poignard P, Sabbe R, Picchio GR, Wang M, Gulizia RJ, Katinger H, Parren PW, Mosier DE, Burton DR.** 1999. Neutralizing antibodies have limited effects on the control of established HIV-1 infection in vivo. Immunity **10:**431–438. http://dx.doi.org/10.1016/S1074-7613(00)80043-6.
54. **Abela IA, Reynell L, Trkola A.** 2010. Therapeutic antibodies in HIV treatment—classical approaches to novel advances. Curr Pharm Des **16:**3754–3766. http://dx.doi.org/10.2174/138161210794079245.
55. **Mehandru S, Vcelar B, Wrin T, Stiegler G, Joos B, Mohri H, Boden D, Galovich J, Tenner-Racz K, Racz P, Carrington M, Petropoulos C, Katinger H, Markowitz M.** 2007. Adjunctive passive immunotherapy in human immunodeficiency virus type 1-infected individuals treated with antiviral therapy during acute and early infection. J Virol **81:**11016–11031. http://dx.doi.org/10.1128/JVI.01340-07.
56. **Trkola A, Kuster H, Rusert P, Joos B, Fischer M, Leemann C, Manrique A, Huber M, Rehr M, Oxenius A, Weber R, Stiegler G, Vcelar B, Katinger H, Aceto L, Gunthard HF.** 2005. Delay of HIV-1 rebound after cessation of antiretroviral therapy through passive transfer of human neutralizing antibodies. Nat Med **11:**615–622. http://dx.doi.org/10.1038/nm1244.
57. **Klein F, Halper-Stromberg A, Horwitz JA, Gruell H, Scheid JF, Bournazos S, Mouquet H, Spatz LA, Diskin R, Abadir A, Zang T, Dorner M, Billerbeck E, Labitt RN, Gaebler C, Marcovecchio PM, Incesu RB, Eisenreich TR, Bieniasz PD, Seaman MS, Bjorkman PJ, Ravetch JV, Ploss A, Nussenzweig MC.** 2012. HIV therapy by a combination of broadly neutralizing antibodies in humanized mice. Nature **492:**118–122. http://dx.doi.org/10.1038/nature11604.
58. **Barouch DH, Whitney JB, Moldt B, Klein F, Oliveira TY, Liu J, Stephenson KE, Chang HW, Shekhar K, Gupta S, Nkolola JP, Seaman MS, Smith KM, Borducchi EN, Cabral C, Smith JY, Blackmore S, Sanisetty S, Perry JR, Beck M, Lewis MG, Rinaldi W, Chakraborty AK, Poignard P, Nussenzweig MC, Burton DR.** 2013. Therapeutic efficacy of potent neutralizing HIV-1-specific monoclonal antibodies in SHIV-infected rhesus monkeys. Nature **503:**224–228. http://dx.doi.org/10.1038/nature12744.
59. **Julien JP, Cupo A, Sok D, Stanfield RL, Lyumkis D, Deller MC, Klasse PJ, Burton DR, Sanders RW, Moore JP, Ward AB, Wilson IA.** 2013.

Crystal structure of a soluble cleaved HIV-1 envelope trimer. Science **342:** 1477–1483. http://dx.doi.org/10.1126/science.1245625.

60. **Lyumkis D, Julien JP, de Val N, Cupo A, Potter CS, Klasse PJ, Burton DR, Sanders RW, Moore JP, Carragher B, Wilson IA, Ward AB.** 2013. Cryo-EM structure of a fully glycosylated soluble cleaved HIV-1 envelope trimer. Science **342:**1484–1490. http://dx.doi.org/10.1126/science.1245627.
61. **Bartesaghi A, Merk A, Borgnia MJ, Milne JL, Subramaniam S.** 2013. Prefusion structure of trimeric HIV-1 envelope glycoprotein determined by cryo-electron microscopy. Nat Struct Mol Biol **20:**1352–1357. http://dx.doi.org/10.1038/nsmb.2711.
62. **Pancera M, Zhou T, Druz A, Georgiev IS, Soto C, Gorman J, Huang J, Acharya P, Chuang GY, Ofek G, Stewart-Jones GB, Stuckey J, Bailer RT, Joyce MG, Louder MK, Tumba N, Yang Y, Zhang B, Cohen MS, Haynes BF, Mascola JR, Morris L, Munro JB, Blanchard SC, Mothes W, Connors M, Kwong PD.** 2014. Structure and immune recognition of trimeric pre-fusion HIV-1 Env. Nature **514:**455–461. http://dx.doi.org/10.1038/nature13808.
63. **Doria-Rose NA, Louder MK, Yang Z, O'Dell S, Nason M, Schmidt SD, McKee K, Seaman MS, Bailer RT, Mascola JR.** 2012. HIV-1 neutralization coverage is improved by combining monoclonal antibodies that target independent epitopes. J Virol **86:**3393–3397. http://dx.doi.org/10.1128/JVI.06745-11.
64. **Goo L, Jalalian-Lechak Z, Richardson BA, Overbaugh J.** 2012. A combination of broadly neutralizing HIV-1 monoclonal antibodies targeting distinct epitopes effectively neutralizes variants found in early infection. J Virol **86:**10857–10861. http://dx.doi.org/10.1128/JVI.01414-12.
65. **Bonsignori M, Hwang KK, Chen X, Tsao CY, Morris L, Gray E, Marshall DJ, Crump JA, Kapiga SH, Sam NE, Sinangil F, Pancera M, Yongping Y, Zhang B, Zhu J, Kwong PD, O'Dell S, Mascola JR, Wu L, Nabel GJ, Phogat S, Seaman MS, Whitesides JF, Moody MA, Kelsoe G, Yang X, Sodroski J, Shaw GM, Montefiori DC, Kepler TB, Tomaras GD, Alam SM, Liao HX, Haynes BF.** 2011. Analysis of a clonal lineage of HIV-1 envelope V2/V3 conformational epitope-specific broadly neutralizing antibodies and their inferred unmutated common ancestors. J Virol **85:**9998–10009. http://dx.doi.org/10.1128/JVI.05045-11.
66. **deCamp A, Hraber P, Bailer RT, Seaman MS, Ochsenbauer C, Kappes J, Gottardo R, Edlefsen P, Self S, Tang H, Greene K, Gao H, Daniell X, Sarzotti-Kelsoe M, Gorny MK, Zolla-Pazner S, LaBranche CC, Mascola JR, Korber BT, Montefiori DC.** 2014. Global panel of HIV-1 Env reference strains for standardized assessments of vaccine-elicited neutralizing antibodies. J Virol **88:**2489–2507. http://dx.doi.org/10.1128/JVI.02853-13.
67. **Doria-Rose N, Bailer R, Louder M, Lin C-L, Turk E, Laub L, Longo N, Connors M, Mascola J.** 2013. High throughput HIV-1 microneutralization assay. Protoc Exch http://dx.doi.org/10.1038/protex.2013.069.
68. **Sarzotti-Kelsoe M, Bailer RT, Turk E, Lin CL, Bilska M, Greene KM, Gao H, Todd CA, Ozaki DA, Seaman MS, Mascola JR, Montefiori DC.** 2014. Optimization and validation of the TZM-bl assay for standardized assessments of neutralizing antibodies against HIV-1. J Immunol Methods **409:**131–146. http://dx.doi.org/10.1016/j.jim.2013.11.022.
69. **Chou TC.** 2006. Theoretical basis, experimental design, and computerized simulation of synergism and antagonism in drug combination studies. Pharmacol Rev **58:**621–681. http://dx.doi.org/10.1124/pr.58.3.10.
70. **Walker LM, Simek MD, Priddy F, Gach JS, Wagner D, Zwick MB, Phogat SK, Poignard P, Burton DR.** 2010. A limited number of antibody specificities mediate broad and potent serum neutralization in selected HIV-1 infected individuals. PLoS Pathog **6:**e1001028. http://dx.doi.org/10.1371/journal.ppat.1001028.
71. **Doria-Rose NA, Klein RM, Daniels MG, O'Dell S, Nason M, Lapedes A, Bhattacharya T, Migueles SA, Wyatt RT, Korber BT, Mascola JR, Connors M.** 2010. Breadth of human immunodeficiency virus-specific neutralizing activity in sera: clustering analysis and association with clinical variables. J Virol **84:**1631–1636. http://dx.doi.org/10.1128/JVI.01482-09.
72. **Mascola JR, Louder MK, VanCott TC, Sapan CV, Lambert JS, Muenz LR, Bunow B, Birx DL, Robb ML.** 1997. Potent and synergistic neutralization of human immunodeficiency virus (HIV) type 1 primary isolates by hyperimmune anti-HIV immunoglobulin combined with monoclonal antibodies 2F5 and 2G12. J Virol **71:**7198–7206.
73. **Zwick MB, Wang M, Poignard P, Stiegler G, Katinger H, Burton DR, Parren PW.** 2001. Neutralization synergy of human immunodeficiency virus type 1 primary isolates by cocktails of broadly neutralizing antibodies. J Virol **75:**12198–12208. http://dx.doi.org/10.1128/JVI.75.24.12198-12208.2001.
74. **Verrier F, Nadas A, Gorny MK, Zolla-Pazner S.** 2001. Additive effects characterize the interaction of antibodies involved in neutralization of the primary dualtropic human immunodeficiency virus type 1 isolate 89.6. J Virol **75:**9177–9186. http://dx.doi.org/10.1128/JVI.75.19.9177-9186.2001.
75. **Bouvin-Pley M, Morgand M, Meyer L, Goujard C, Moreau A, Mouquet H, Nussenzweig M, Pace C, Ho D, Bjorkman PJ, Baty D, Chames P, Pancera M, Kwong PD, Poignard P, Barin F, Braibant M.** 2014. Drift of the HIV-1 envelope glycoprotein gp120 toward increased neutralization resistance over the course of the epidemic: a comprehensive study using the most potent and broadly neutralizing monoclonal antibodies. J Virol **88:**13910–13917. http://dx.doi.org/10.1128/JVI.02083-14.
76. **Hessell AJ, Rakasz EG, Tehrani DM, Huber M, Weisgrau KL, Landucci G, Forthal DN, Koff WC, Poignard P, Watkins DI, Burton DR.** 2010. Broadly neutralizing monoclonal antibodies 2F5 and 4E10 directed against the human immunodeficiency virus type 1 gp41 membrane-proximal external region protect against mucosal challenge by simian-human immunodeficiency virus SHIVBa-L. J Virol **84:**1302–1313. http://dx.doi.org/10.1128/JVI.01272-09.
77. **Shingai M, Donau OK, Plishka RJ, Buckler-White A, Mascola JR, Nabel GJ, Nason MC, Montefiori D, Moldt B, Poignard P, Diskin R, Bjorkman PJ, Eckhaus MA, Klein F, Mouquet H, Cetrulo Lorenzi JC, Gazumyan A, Burton DR, Nussenzweig MC, Martin MA, Nishimura Y.** 2014. Passive transfer of modest titers of potent and broadly neutralizing anti-HIV monoclonal antibodies block SHIV infection in macaques. J Exp Med **211:**2061–2074. http://dx.doi.org/10.1084/jem.20132494.
78. **Shibata R, Igarashi T, Haigwood N, Buckler-White A, Ogert R, Ross W, Willey R, Cho MW, Martin MA.** 1999. Neutralizing antibody directed against the HIV-1 envelope glycoprotein can completely block HIV-1/SIV chimeric virus infections of macaque monkeys. Nat Med **5:**204–210. http://dx.doi.org/10.1038/5568.
79. **Mascola JR, Lewis MG, Stiegler G, Harris D, VanCott TC, Hayes D, Louder MK, Brown CR, Sapan CV, Frankel SS, Lu Y, Robb ML, Katinger H, Birx DL.** 1999. Protection of macaques against pathogenic simian/human immunodeficiency virus 89.6PD by passive transfer of neutralizing antibodies. J Virol **73:**4009–4018.
80. **Hessell AJ, Rakasz EG, Poignard P, Hangartner L, Landucci G, Forthal DN, Koff WC, Watkins DI, Burton DR.** 2009. Broadly neutralizing human anti-HIV antibody 2G12 is effective in protection against mucosal SHIV challenge even at low serum neutralizing titers. PLoS Pathog **5:**e1000433. http://dx.doi.org/10.1371/journal.ppat.1000433.
81. **Nishimura Y, Igarashi T, Haigwood N, Sadjadpour R, Plishka RJ, Buckler-White A, Shibata R, Martin MA.** 2002. Determination of a statistically valid neutralization titer in plasma that confers protection against simian-human immunodeficiency virus challenge following passive transfer of high-titered neutralizing antibodies. J Virol **76:**2123–2130. http://dx.doi.org/10.1128/jvi.76.5.2123-2130.2002.
82. **Hessell AJ, Hangartner L, Hunter M, Havenith CE, Beurskens FJ, Bakker JM, Lanigan CM, Landucci G, Forthal DN, Parren PW, Marx PA, Burton DR.** 2007. Fc receptor but not complement binding is important in antibody protection against HIV. Nature **449:**101–104. http://dx.doi.org/10.1038/nature06106.